Desorption of cluster ions from solid Ne by low energy ion impact

T. Tachibana[1]‡, K. Fukai[2], T. Koizumi[1,2], T. Hirayama[1,2]

[1]Research Center for Measurement in Advanced Science (RCMAS), Rikkyo University, Toshima-ku, Tokyo 171-8501, Japan

[2]Department of Physics, Rikkyo University, Toshima-ku, Tokyo 171-8501, Japan

E-mail: `hirayama@rikkyo.ac.jp`

Abstract. We investigated Ne^+ ions and Ne_n^+ ($n = 2 - 20$) cluster ions desorbed from the surface of solid Ne by 1.0 keV Ar^+ ion impact. Kinetic energy analysis shows a considerably narrower energy distribution for the Ne_n^+ ($n \geq 3$) ions than for the Ne_n^+ ($n = 1, 2$) ions. The dependence of ion yields on Ne film thickness indicates that cluster ions ($n \geq 3$) are desorbed only from relatively thick films. We conclude that desorbed ions grow into large cluster ions during the outflow of deep bulk atoms to the vacuum.

PACS numbers: 79.20.Rf

‡ Present address: Department of Physics, Tokyo University of Science, 1-3 Kagurazaka, Shinjuku-ku, Tokyo 162-8601, Japan

1. Introduction

The interaction of ions with solids has been studied extensively both experimentally and theoretically for many years [1–3]. The desorption of ions and neutrals from solid surfaces stimulated by energetic ion impact is a well-known phenomenon that has numerous applications in science and engineering fields. Depending on the target species and projectile energy, several different desorption models have been proposed.

A general interpretation of the desorption mechanism that occurs upon keV ion impact is referred to as kinetic sputtering, which involves the process of momentum transfer to secondary and higher-order recoiling target atoms. The momentum transfer occurs as the collision cascade in the target propagates back to the surface, a result of which may be the sputtering (desorption) of the target species. Sigmund [4] proposed a linear collision cascade model based on linear Boltzmann transport theory. Working within the linear collision cascade regime, this model assumes that a target atom at rest is displaced by a collision with a moving atom. The model has been shown to provide a satisfactory description of the kinetic sputtering process. Another model emphasizes the role of a non-linear spike (i.e., a dense collision cascade) generated by high-energy or heavy ion impact [1, 5, 6]. In this model, the linear collision cascade model is no longer valid because most of the atoms in the spike regime are assumed to be in motion. Spike effects become pronounced for very weakly bound condensed gas targets, even when stimulated by ion impacts of several keV or less [7–9]. The total desorption yield (the average number of sputtered species per incident ion) for condensed rare gas solids is surprisingly large, representing an effect that cannot be explained using only the linear collision cascade model [10, 11]. Urbassek and Michel [12] proposed a gas flow model for condensed rare gas solids. According to this model, the target surface is disrupted by a large pressure buildup in the gaseous core of the spike volume, following which a large number of atoms begin to flow out into the vacuum. Such a scenario is consistent with the evolution of the molecular dynamics simulated for solid Ar impacted by 1.0 keV neutral Ar [13, 14]. It has also been recognized that electronic excitation at the surface layers stimulated by primary ions or outgoing secondary electrons can result in the desorption of neutrals and ions from the surface. The basic mechanisms by which the electronic excitation energy is converted into kinetic energy of the desorbed species are discussed in detail in the literature [15–17].

Some studies have focused on the formation mechanisms of secondary ions. In particular, one of the characteristic features of this mechanism is very efficient desorption of large cluster ions from condensed gas solids. For example, Michel and coworkers [18] reported on Ar_n^+ ($n = 1 - 26$) ions desorbed from thick Ar films by 3.5 keV Ar^+ impact. The authors also observed cluster ions desorbed from simple molecular solids [19]. They inferred that these large cluster ions are formed and desorbed during the gas flow process [7]. Baba and coworkers [20, 21] studied cluster ion desorption from condensed CH_4 and N_2 solids by He^+ ion impact. When solid targets are stimulated by light ions, the projectile energy is significantly consumed by inelastic collisions, resulting

in electronic excitations of the target atoms. The authors suggested that evaporation from the target surface following high-density electronic excitation leads to cluster ion formation and desorption. Secondary ions from Ar/Xe, Ar/N_2, and Ar/O_2 mixtures stimulated by 0.4 keV He^+ ion impact were investigated previously by Hiraoka *et al* [22]. The authors measured the dependence of the mixing ratio on the desorbed ion yield and discussed the relaxation processes of electronic excitations that lead to the observed atomic and small cluster ion desorption. However, large rare gas cluster ions desorbed by light ion impact have not been observed in the secondary ion mass spectra [7, 18, 20]. Although the formation and desorption of large clusters from rare gas solids are strongly influenced by momentum transfer processes within the target solids, the mechanism of formation and desorption remains incompletely understood.

In the present paper, we investigate ions desorbed from solid Ne by 1.0 keV Ar^+ impact. For comparison, we also present the results for the desorbed neutrals and ions resulting from ion impact and low-energy electron irradiation, respectively. Based on the mass spectra, the kinetic energy distribution of the desorbed ions, and the dependence of yield on sample thickness, we discuss the formation and desorption mechanisms of cluster ions.

2. Experimental

Detail of the experimental apparatus has been published elsewhere [23, 24]. Briefly, the experiments were carried out in a UHV chamber with a base pressure of 8×10^{-9} Pa and equipped with a closed-cycle helium cryostat. The ions were generated by a 10 GHz electron cyclotron resonance ion source (Nanogan, Pantechnik). The ion beam was introduced into the UHV chamber using electrostatic lenses after passing through a magnetic field to select the appropriate mass/charge state. A copper substrate was fixed to the cryostat and cooled to approximately 4.9 K, and the substrate was electrically grounded during the measurements. Pure Ne was condensed on the substrate by filling the chamber with Ne gas to a pressure of $10^{-6} - 10^{-4}$ Pa.

The sample thickness was estimated from the exposure, assuming a condensation coefficient of unity. The rare gas surface was impacted by 1.0 keV Ar^+ ions at an incidence angle of 60 degrees with respect to the surface-normal and the ions desorbed perpendicular to the surface were detected by means of a quadrupole mass spectrometer (QMS, ULVAC MSQ-400) operating in a pulse counting mode.

The incident ion beam current was monitored by a movable Faraday cup in front of the sample surface. To minimize sample damage due to ion impact, the ion beam current was kept below 0.5 nA. The kinetic energy distribution of the desorbed ions was analyzed by placing a 4-grid-type retarding field energy analyzer in front of the entrance to the QMS.

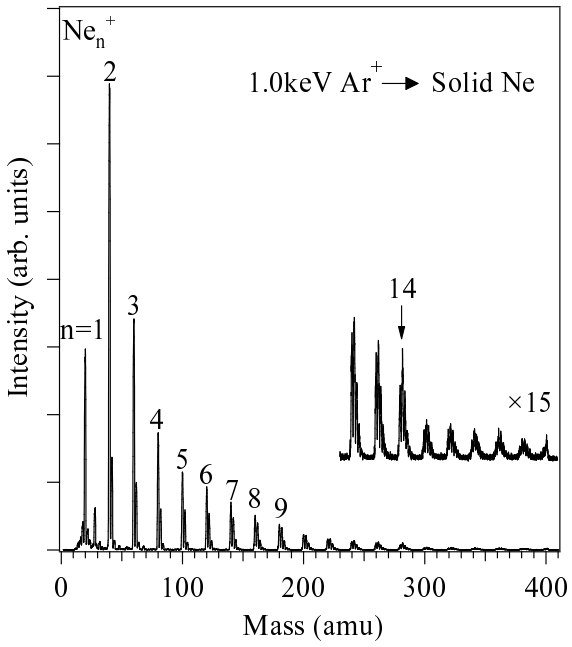

Figure 1. Mass spectrum of ions desorbed from solid Ne (500 ML) by 1.0 keV Ar^+ impact. Sample temperature was 4.9 K.

3. Mass spectra

The mass spectrum of ions desorbed from the surface of solid Ne by 1.0 keV Ar^+ impact is shown in Fig. 1. The sample thickness was 500 mono-layers (ML). Peaks are observed corresponding to Ne^+ ions and Ne_n^+ cluster ions with a cluster size n from 2 to 20. The time that it takes for the desorbed ions to reach the detector is a few microseconds, and the desorbed cluster ions may undergo structural rearrangement and fragmentation within the time [25]. Although the largest observable cluster size ($n = 20$) is limited in the experiment described herein by the range of used in the present QMS ($M_{max} = 400$ amu), the Ne_n^+ ions up to a size of $n > 100$ were measured in our previous experiments using a time-of-flight technique [23]. The cluster ion signal intensity decreases exponentially with cluster size, but the existence of a discontinuity in the signal intensity at size n=14 to 15 is confirmed (see Fig. 1). Because the Ne_{14}^+ ion is predicted to have an icosahedral structure with a dimer ion core [26] it is likely that this discontinuity reflects the structure stability of the cluster ions, which depends on the cluster size.

We also measured the mass spectrum of particles desorbed by 300 eV electron irradiation (Fig. 2(a)). A mechanism based on inter-atomic charge transfer leading to Coulomb repulsion between neighboring ions has been proposed to account for ion desorption induced by electronic transitions (DIET) from the surface of rare gas solids [27]. Recent studies have reported low-energy electron- or photon-stimulated desorption by Coulomb repulsion of large cluster ions ($n \geq 8$) from molecules adsorbed

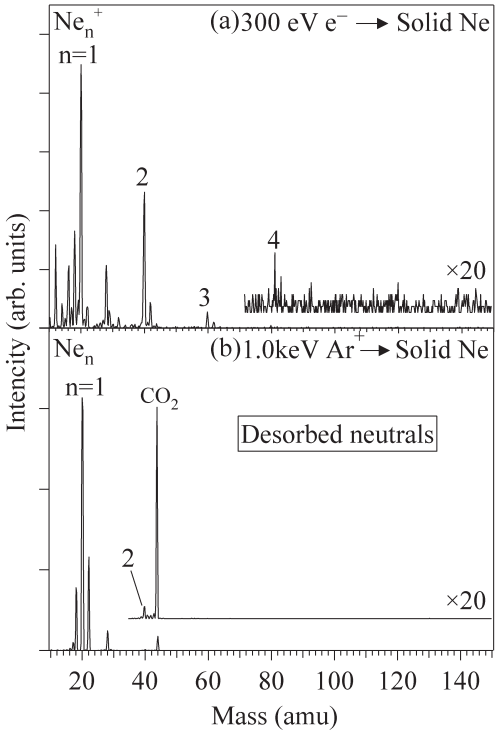

Figure 2. (a) Mass spectrum of ions desorbed from solid Ne (500 ML) by 300 eV electron irradiation. (b)Mass spectrum of neutrals desorbed from solid Ne (500 ML) by 1.0 keV Ar^+ impact. The desorbed neutrals were detected following their ionization by 70 eV electrons in the QMS ionizer. Note that residual gas molecules were also detected at $M/e = 18(H_2O)$, $28(CO_2)$, and $44(CO_2)$. Sample temperature was 4.9 K.

on condensed gas solids [28–31]. However, the results in Fig. 2(a) show that the monomer peak dominates and that only very small cluster ions are observed ($n < 5$). This result indicates that desorption of large cluster ions from pure solid Ne has no relevance to the DIET process. Instead, we consider that collisions between the impacting projectile and the target atom trigger the desorption of the large rare gas cluster ions.

The mass spectrum of neutrals desorbed by 1.0 keV Ar^+ impact is shown in Fig. 2(b). Note that residual gas molecules are also detected at $M/e = 18(H_2O)$, $28(CO_2)$, and $44(CO_2)$. If momentum transfer leads to desorption via kinetic sputtering of large cluster ions, then desorbed species including neutral clusters should be observed; however, the mass pattern of the neutrals differs from that of the ions. Even though the majority of the desorbed species are known to be neutrals, there is no signal from desorbed neutral Ne clusters, except for a relatively weak signal from the Ne dimer. This observation suggests that cluster ions are not formed directly in solid Ne. To explain the formation process of large cluster ions, we must consider the clustering reaction between ions and atoms after the kinetic sputtering process. Here, our recent experimental result is helpful in discussing the clustering process. In particular, the total desorption yield of solid Ne (500ML) for 1.0 keV Ar^+ impact with perpendicular incidence is estimated

to be ∼3000 atoms/ion [24]. This extremely large yield leads us to propose that large cluster ions are grown in the desorption flux, as the desorbing ion has the possibility to react with a large number of surrounding atoms.

4. Kinetic energy distribution

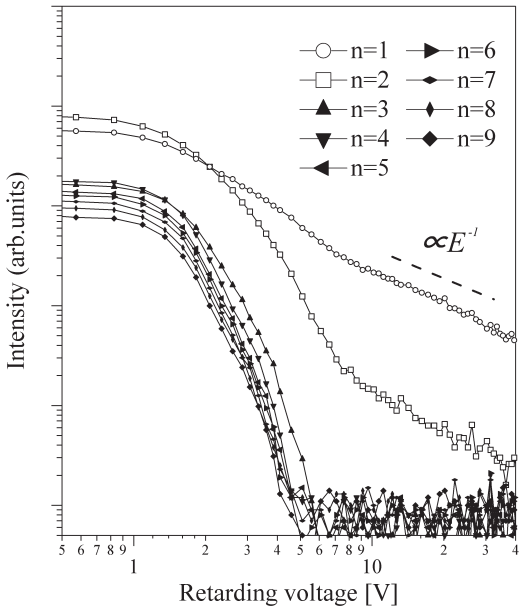

Figure 3. Retardation plots of Ne_n^+ $(n = 1-9)$ ions desorbed from solid Ne (120 ML) by 1.0 keV Ar^+ impact. Sample temperature was 4.9 K.

Kinetic energy measurements of the desorbing species is a useful method for studying the fundamentals of the desorption mechanism; however, quantitative measurement of the ion energy is difficult because of effects such as the contact potential and charge-up effect. In addition, the ion energy distribution is related to the ionization and neutralization probabilities, which should depend on the desorbing ion and its velocity. Unfortunately, these dependencies are poorly understood, at least for condensed rare gas targets, thus, a detailed theoretical analysis of the ion energy distribution remains a difficult challenge. Nevertheless, it is possible to find traces of the desorption process in the characteristic behaviors and features of the ion energy distribution [32–37].

Retardation plots of Ne_n^+ $(n = 1-9)$ ions desorbed from solid Ne (120 ML) by Ar^+ impact are shown in Fig. 3. The voltage shifts for the charge-up and the contact potential are not corrected. The integrated kinetic energy spectrum depends on the cluster size: the Ne_n^+ $(n = 3-9)$ ions have a considerably narrower energy distribution compared with the Ne_n^+ $(n = 1, 2)$ ions. The kinetic energy distribution for the Ne_n^+ $(n = 3-9)$ ions are all similar, suggesting that these ions are formed and desorbed via

the same process. In contrast, the kinetic energy distribution for the Ne_n^+ $(n = 1, 2)$ ions has a high-energy tail. The low-energy end of the distribution, however, is somewhat similar to that observed for Ne_n^+ $(n = 3-9)$ ions. This observation implies that different processes are involved in the desorption of Ne_n^+ $(n = 1, 2)$ and Ne_n^+ $(n = 3 - 9)$ ions.

The energy distribution of the desorbed species is frequently compared to the Sigmund-Thompson formula, which is derived assuming that desorbed atoms originate in a linear collision cascade process [4]. Explicitly,

$$f(e) \propto \frac{e}{(e + U_0)^3}, \tag{1}$$

where U_0 is the surface binding energy and e is the kinetic energy of the desorbed particle. Commonly, the cohesive energy of the target (Ne; 0.02 eV) is used to U_0. The integrated kinetic energy distribution derived from equation (1) is given by

$$\int_\infty^E f(e)de \propto \frac{2E + U_0}{(E + U_0)^2}, \tag{2}$$

where E denotes the retarding potential. According to this formula, the high-energy part of the integrated energy distribution falls off as E^{-1}. Our experimental results for the high-energy side of the Ne^+ ion distribution are in reasonable agreement with the theoretical asymptotic behavior, $\propto E^{-1}$ (dashed line in Fig. 3). Similar behavior is also found in the dimer ion distribution. This analysis supports the conclusion that high-energy ions are desorbed via the linear collision cascade process.

As stated above, our interpretation is that low-energy ions and cluster ions are desorbed via one or more processes that differ from the linear collision cascade process. For neutral desorption from rare gas solids, the desorption mechanism has been explained by a combination of the linear and non-linear spike models [9, 13, 14]. If rare gas ions are desorbed via processes similar to neutral sputtering, it remains possible that the driving force for desorption of low-energy ions and cluster ions originates from the non-linear spike process. In addition, the fact that the total desorption yield by keV ion impact from rare gas solids is much larger than that estimated by the linear collision cascade theory has been attributed to enhancement in the yield of the non-linear spike [8–14]. It might also be inferred that the efficient desorption of cluster ions is relevant to the non-linear spike process.

5. Thickness dependence

The desorption yields of Ne_n^+ $(n = 1 - 12)$ ions as a function of film thickness are shown in Fig. 4. The longitudinal range of the incident 1.0 keV Ar ion is estimated by SRIM2008 [38] to be 3.4 nm, which correspond to about 13 ML of solid Ne. For Ne films less than ∼10 ML thick, only monomer and dimer ions are desorbed. The yields for the Ne_n^+ $(n = 3 - 12)$ ions increase above ∼20 ML, causing the cluster size distribution to shift toward the large sizes with increasing Ne film thickness. The ion yield tends to saturation at an Ne film thickness of ∼300 ML, implying that the cluster ion desorption process is connected with collision or spike regime in the deep bulk. In contrast, in

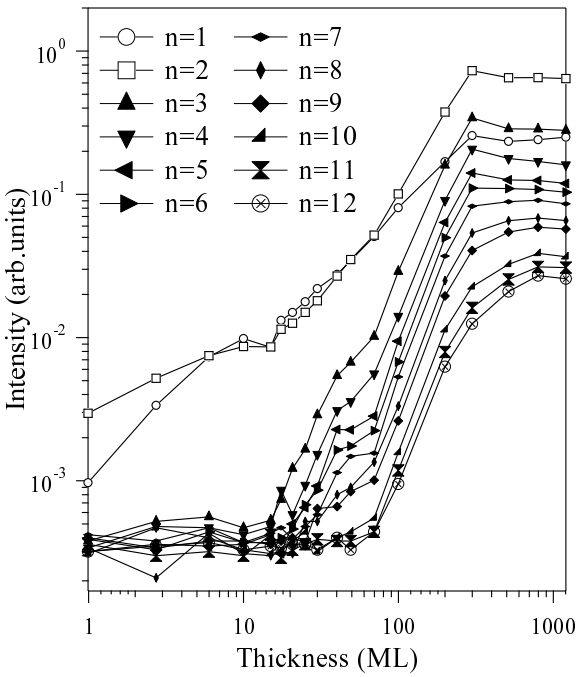

Figure 4. Desorption yields of Ne_n^+ $(n = 1 - 12)$ ions induced by 1.0 keV Ar^+ impact as a function of Ne film thickness. Sample temperature was 4.9 K.

the very low coverage regime (>∼10 ML) the Ne_n^+ $(n = 1, 2)$ ions may originate at the target surface or from adsorbed atoms on the Cu substrate. These results suggest that small ions can be desorbed via the linear collision cascade process and/or the DIET process. The fact that for thick Ne films the Ne_n^+ $(n = 1, 2)$ ion yields increase in the same manner as the Ne_n^+ $(n = 3-12)$ ion yields suggests that most of the Ne_n^+ $(n = 1, 2)$ ions in this thickness regime are desorbed via the same process as that applicable to the large cluster ions.

6. Desorption model

For condensed gas targets, the non-linear spike effect is predicted by the gas flow model [12]. In this model, the surface is disrupted and a large number of atoms are desorbed from inside the target due to gasification of a certain part of the spike volume. Based on the gas flow model and our experimental results, we propose the following interpretation of the desorption mechanism for large cluster ions. During the outflow of a large number of bulk atoms into the vacuum, a desorbing ion from the spike volume may grow into a large cluster ion by three-body collisions with surrounding neutral atoms. Explicitly,

$$Ne_n^+ + 2Ne \rightarrow Ne_{n+1}^+ + Ne. \tag{3}$$

Because the outflow gas density increases within the spike regime in solid Ne, the growth reaction rate and the desorption yields of cluster ions should increase with

increasing Ne film thickness. When the thickness of the solid Ne is comparable with the depth of the spike regime, the desorption yields become saturated.

7. Summary

We observed Ne^+ and cluster ions, Ne_n^+ $(n = 2 - 20)$, desorbing from solid Ne due to 1.0 keV impacts. The kinetic energy distribution of desorbed Ne_n^+ $(n \geq 3)$ ions is considerably narrower than that of Ne_n^+ $(n = 1, 2)$ ions. The high-energy side in the kinetic energy distribution of Ne_n^+ $(n = 1, 2)$ ions can be explained by the linear collision cascade process. The results of an investigation of the dependence of the desorbed ion yield on film thickness reveal that cluster ions $(n \geq 3)$ are desorbed effectively only from relatively thick films. We suggest that a desorbing ion grows into a large cluster ion by three-body collisions with surrounding neutral atoms during the outflow of a large number of bulk atoms into the vacuum via the gas flow process.

8. Acknowledgments

This work was partly supported by a Grant-in-Aid for Scientific Research from MEXT (Ministry of Education, Culture, Sports, Science and Technology) and by the Rikkyo University Special Fund for Research.

9. References

[1] Behrisch R (ed) 1981 *Sputtering by Particle Bombardment I: Physical sputtering of single element solids* (Springer, Berlin)
[2] Sigmund P 1987 *Nucl. Instr. Meth Phys. Res. B* **27** 1
[3] Behrisch R and Eckstein W (eds) 2007 *Sputtering by Particle bombardment: Experiments and Computer Calculations from Threshold to Mev Energies* (Springer, Berlin)
[4] Sigmund P 1969 *Phys. Rev.* **184** 383
[5] Oostra D, van Ingen R, Haring A, de Vries A and Saris F 1988 *Phys. Rev. Lett.* **19** 1392
[6] Szymónski M and Postawa Z 1990 *Appl. Phys.* **50** 269
[7] David D, Magnera T, Tian R, Stulik D and Michl J 1986 *Nucl. Instr. Meth Phys. Res. B* **14** 378
[8] Ellegaard O, Shou J, Stenum B, Sørensen H and Pedrays R 1992 *Nucl. Instr. Meth Phys. Res. B* **62** 447
[9] Pedrys R, Warczak B, Leskiewicz P, Schou J and Ellegaard1999 O 1999 *Nucl. Instr. Meth Phys. Res. B* **157** 121
[10] Brawn W L and Johnson R 1986 *Nucl. Instr. Meth Phys. Res. B* **13** 295
[11] Balaji V, David D, Magnera T, Michl J and Urabassek H 1990 *Nucl. Instr. Meth Phys. Res. B* **46** 435
[12] Urbassek H and Michl J 1987 *Nucl. Instr. Meth Phys. Res. B* **22** 480
[13] Urbassek H and Waldeer K 1991 *Phys. Rev. Lett.* **67** 105
[14] Waldeer K and Urbassek H 1993 *Nucl. Instr. Meth Phys. Res. B* **73** 14
[15] Ellegaard O, Schou J and Sørensen H 1986 *Nucl. Instr. Meth Phys. Res. B* **13** 567
[16] Schou J 1987 *Nucl. Instr. Meth Phys. Res. B* **27** 188
[17] Hirayama T and Arakawa I 2006 *J. Phys. Cond. Matt.* **18** 1563
[18] Orth R, Jonkman H, Powell D and Michl J 1981 *J. Am. Chem. Soc.* **20** 6026
[19] Orth R, Jonkman H and Michl J 1982 *Int. J. Mass Spectrom. Ion Phys.* **43** 41

[20] Baba Y, Sekiguchi T and Shimoyama I 2005 *Surf. Sci.* **593** 324
[21] Narita A, Honda M, Hirao N, Baba Y and Yaita T 2008 *Appl. Surf. Sci.* **255** 883
[22] Hiraoka K, Hamamoto R, Mori K, Watanabe M and Sato T 2002 *Int. J. Mass Spectrum.* **218** 173
[23] Fukai K, Fujita S, Tachibana T, Koizumi T and Hirayama T 2010 *J. Phys. Cond. Matt.* **22** 084007
[24] Fujita S, Tachibana T, Koizumi T and Hirayama T 2010 *J. Phys., Conf. Ser.* **22** 084007
[25] Dzhemilev N, Rasulev U, Verkhoturov S 1987*Nucl. Instr. Meth Phys. Res. B* **29** 531
[26] Märk T and Scheier P 1987 *Chem. Phys. Lett.* **12** 245
[27] Dujardin G, Hellner L, Besnard-Ramage M and Azria R 1990 *Phys. Rev. Lett.* **64** 1289
[28] Souda R 2002 *Surf. Sci. Lett.* **506** L275
[29] Souda R 2003 *Chem. Phys. Lett.* **382** 387
[30] Tachibana T, Yamauchi Y, Miura T, Hirayama T, Sakurai M and Arakawa I 2005 *Surf. Sci.* **593** 264
[31] Tachibana T, Miura T and Arakawa I 2006 *Low. Temp. Phys.* **32** 1434
[32] Wang L, Nor R and Graham W 1997 *J. Phys. D* **30** 2379
[33] Williams P 1981 *Phys. Rev. B* **23** 6187
[34] Pereira J and Silveira E 1997 *Surf. Sci.* **390** 158
[35] Pereira J, Bitensky I and da Silveira E 1998 *Int. J. Mass Spectrom. Ion Proc.* **174** 179
[36] Souda R 2003 *J. Chem. Phys.* **114** 1823
[37] Bouneau S, Negra S D, Jacquet D, Beyec Y L, Pautrat M, Shapiro M and Tombrello T 2005 *Phys. Rev. B* **71** 174110
[38] Ziegler J F 2005 Computer codes SRIM-2008, http://www.srim.org/